Earthline Journal of Chemical Sciences
E-ISSN: 2581-9003; CODEN: EJCSB4
Volume 13, Number 3, August 2026, Pages 327-340
https://doi.org/10.34198/ejcs.13326.23.327340

Interaction of zinc cation with captopril – A DFT treatment

Lemi Türker

Department of Chemistry, Middle East Technical University, Üniversiteler, Eskişehir Yolu No: 1, 06800 Çankaya/Ankara, Turkey
e-mail: lturker@gmail.com; lturker@metu.edu.tr

Abstract

Zinc has a great potential value in human metabolism. Zinc cation incorporates in many enzyme structures. Captopril is an antihypertensive medicine whose hypotensive activity may result from an inhibitory action on renin-angiotensin system. Presently, interaction of zinc cation with captopril has been considered within the constraints of density functional theory at the level of B3LYP/6-31+G(d). The collected data have revealed that the optimized structures of the species considered have exothermic heats of formation and favorable Gibbs free energy of formation values. They are thermally favored and electronically stable at the standard states. Some electron population has been transferred to the zinc cation and its initial formal charge is no longer +2. On the other hand, doubly charged captopril cation decomposes. Various structural and quantum chemical data have been collected and discussed, including IR and UV-VIS spectra.

1. Introduction

Zinc is one of the most abundant nutritionally essential elements in the human body. In general, it is found in all body tissues such that with 85% of the whole body zinc is in muscle and bone, 11% in the skin and the liver and the rest remains in all the other tissues [1]. Virtually all zinc in multicellular organisms, is intracellular, 30–40% of it is located in the nucleus, 50% in the cytoplasm, organelles and specialized vesicles including digestive enzymes or hormones and the remainder in the cell membrane [1,2]. Zinc intake ranges depending on the source, and human zinc requirement which is estimated at 15 mg/d. Zinc is essential for the structure and function of a large number of macromolecules and for over 300 enzymic reactions [3]. It has both catalytic and structural roles in enzymes, while in zinc finger motifs, it provides a scaffold that organizes protein sub-domains for the interaction with either DNA or other proteins [1,3]. It is critical for the function of a number of metalloproteinase, inducing members of oxido-reductase, hydrolase ligase, lyase family and has co-activating functions with copper in superoxide dismutase or phospholipase C. The zinc ion (Zn^{++}) does not participate in redox reactions, thus it is a stable ion in a biological medium whose potential is in constant flux. Zinc ions are hydrophilic and do not cross cell membranes by passive diffusion [1,2]. In general, transport has been described as having both saturable and non-saturable components, depending on the Zn(II) concentrations involved. Zinc ions exist primarily in the form of complexes with proteins and nucleic acids and participate in all aspects of intermediary metabolism, transmission and regulation of the expression of genetic information, storage, synthesis and action of peptide hormones and structural maintenance of chromatin and biomembranes [1].

Zinc metabolism involves the absorption, distribution, storage, and excretion of zinc, and it is an essential trace element required for protein synthesis, immune function, and genetic expression. The body tightly

Received: July 2, 2026; Accepted: July 27, 2026; Published online: July 31, 2026

Keywords and phrases: captopril, zinc cation, hypotensive agent, density functional calculations, spectra.

regulates homeostasis through two specific transporter families: ZIP proteins (which move zinc into cells) and ZnT proteins (which move zinc out of cells or into organelles) [4]. Zinc and some human diseases are interrelated in many respects [5,6].

On the other hand, Captopril is known as the first orally active inhibitor of angiotensin -converting enzyme to become available [7,8]. It is known that captopril inhibits the converting enzyme peptidyl dipeptidase that hydrolyzes angiotensin I to angiotensin II and inactivates bradykinin, which is a potent vasodilator. The hypotensive activity of captopril may result from an inhibitory action on renin-angiotensin system and a stimulating action on the kallikrein-kinin system [8]. In most of the cases of severe hypertension captopril plus a diuretic usually reduces blood pressure significantly more than it could be achieved with 'standard triple therapy' [7]. Indeed, patients not responding to or not tolerating 'traditional' antihypertensive therapy are the most suitable candidates for captopril treatment. Captopril which is an angiotensin-converting enzyme (ACE) inhibitor, has been widely and effectively used for therapy of arterial hypertension and cardiovascular diseases. However, the protective effects of captopril on hypertension-induced organ damage remain elusive. Although captopril has been well tolerated in most patients, nevertheless some troublesome or potentially serious side effects have been reported. The final place of captopril in the treatment of hypertension may depend on further clarification of its adverse effects [7-9]. Captopril has produced encouraging improvement in some of patients with severe congestive heart failure resistant to conventional therapy [7].

In the past, captopril had been the focus of many researchers including its side effects [7,9-18]. In the present study, interaction of zinc cation with captopril and some other interesting features of it at the molecular level in the realm of density functional theory have been presented.

2. Method of Calculations

In the present study, all the initial optimizations of the structures leading to energy minima have been achieved first by using MM2 method which is then followed by semi empirical PM3 self consistent fields molecular orbital method [19-21]. Afterwards, the structure optimizations have been achieved within the framework of Hartree-Fock and finally by using density functional theory (DFT) at the level of B3LYP/6-31+G(d) [22,23]. This basis set is suitable for zinc. Note that the exchange term of B3LYP consists of hybrid Hartree-Fock and local spin density (LSD) exchange functions with Becke's gradient correlation to LSD exchange [24]. The correlation term of B3LYP consists of the Vosko, Wilk, Nusair (VWN3) local correlation functional [25] and Lee, Yang, Parr (LYP) correlation correction functional [26]. In the present study, the normal mode analysis for each structure yielded no imaginary frequencies for the $3N–6$ vibrational degrees of freedom, where N is the number of atoms in the system. This search has indicated that the structure of each molecule considered corresponds to at least a local minimum on the potential energy surface. Furthermore, all the bond lengths have been thoroughly searched in order to find out whether any bond cleavages occurred or not during the geometry optimization process. All these computations were performed by using SPARTAN 06 program [27].

3. Results and Discussion

In the following paragraphs, captopril is abbreviated as Cap. Figure 1 displays the optimized structures, as well as the directions of the dipole moment vectors of the species presently considered. Notice the decomposed structure of dication of Cap structure (Cap^{+2}). Also note that the presence of the zinc cation causes to change the direction of dipole moment vector of Cap molecule similar to Cap^{+2}.

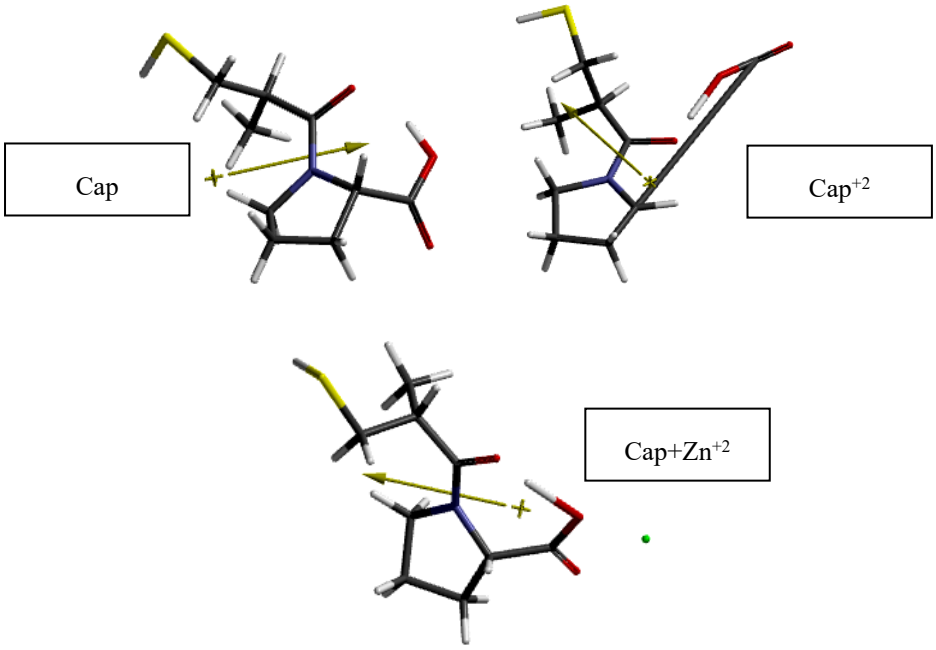

Figure 1. Optimized structures of the species considered (B3LYP/6-31+G(d)).

Table 1 list some thermo chemical properties of the species considered. Data in the table reveal that the standard heat of formation (Hº) values of them are exothermic and they are favored according to their Gº (Gibbs free energy of formation) values.

Table 1. Some thermo chemical properties of the species considered.

Species	Hº	Sº (J/molº)	Gº
Cap	-2705336.869	457.33	-2705473.238
Cap^{+2}	-2703579.552	476.03	-2703721.487
$Cap+Zn^{+2}$	-7374729.045	487.06	-7374874.263

Energies in kJ/mol.

Table 2 shows some energies of the species considered. Note that E, ZPE and E_C stand for the total electronic energy, zero point vibrational energy and the corrected total electronic energy, respectively [27]. The data in Table 2 reveal that optimized structures are all electronically stable structures.

Table 2. Some energies of the species considered.

Species	E	ZPE	E_C
Cap	-2705978.52	631.43	-2705347.09
Cap^{+2}	-2704212.73	621.05	-2703591.68
$Cap+Zn^{+2}$	-7375335.57	636.16	-7374699.41

Energies in kJ/mol.

Figure 2 displays the calculated IR spectrums of the species considered. IR spectrum of Cap has acid COO-H stretch at 3269 cm^{-1}, followed by various C-H stretchings occurring in the region of 3178-3062 cm^{-1}.

The very weak peak at 2720 stands for S-H stretch. The acid C=O stretching happens at 1827 cm^{-1} as a strong peak whereas C=O stretching takes place at 1645 cm^{-1} (Strong). Another moderately strong peak happens at 1468 and is assigned as acid CO-OH bending flanked with some C-H vibrations.

Cap^{+2} is a decomposed structure. Some weak C-H stretchings happen at 3240-3162 cm^{-1}.

IR spectrum of Cap^{+2} possesses O-H stretching of the expelled moiety at 3149 cm^{-1} (very strong). Then, a moderately strong peak comes at 2437 cm^{-1} which belongs to the expelled moiety again.

As for the IR spectrum of $Cap+Zn^{+2}$, COO-H stretch happens at 3396 cm^{-1} as a very weak peak, followed by weak C-H stretchings spread over 3218-3064 cm^{-1}. The S-H stretch occurs at 2721 cm^{-1} (weak). The very strong peak at 1629 cm^{-1} comprises the C=O and C-C stretching and various bending motions.

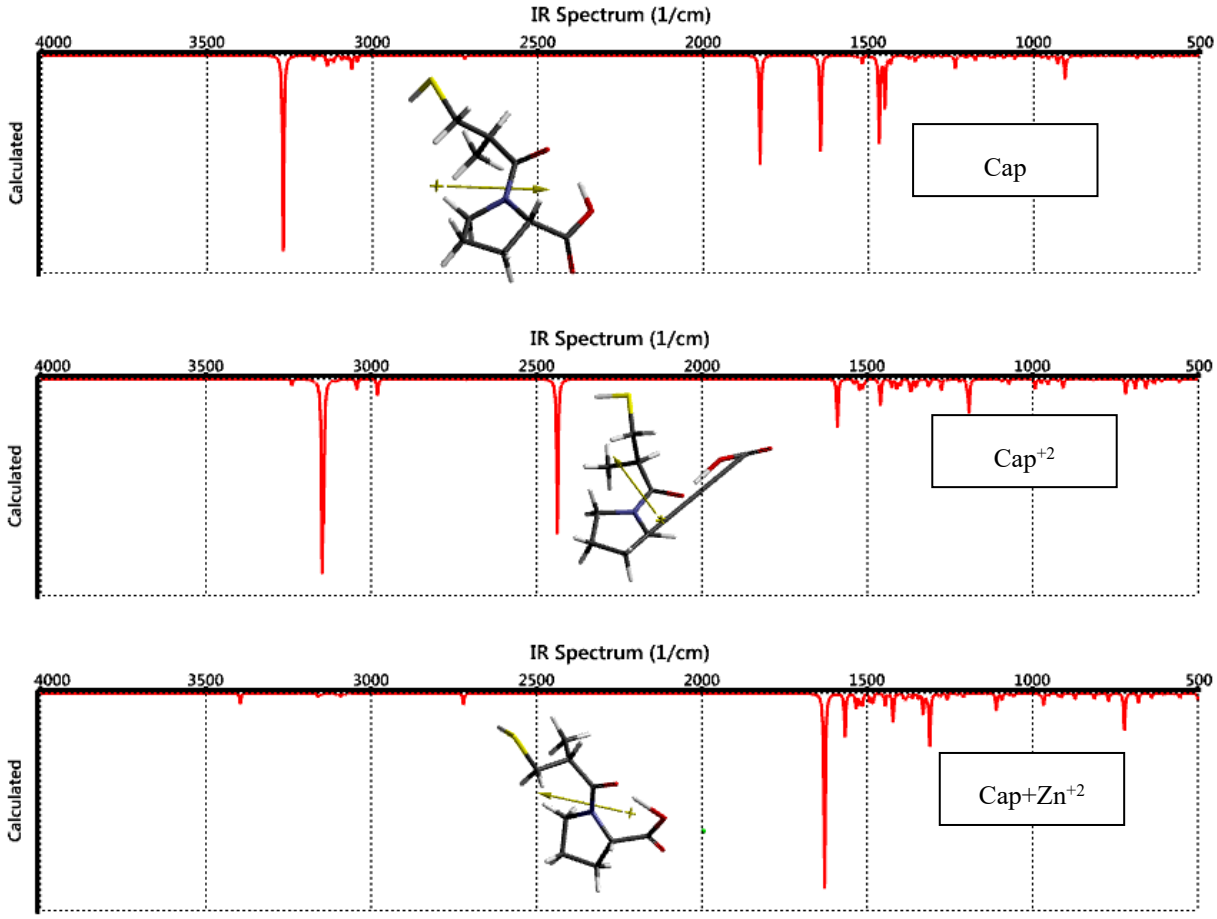

Figure 2. Calculated IR spectrums of the species considered.

The ESP charges are obtained by the program which uses a numerical method that generates charges, thus reproducing the electrostatic potential field from the entire wavefunction [27]. Figure 3 shows the ESP charges on atoms of the species presently considered. In the Cap structure the sulfur atom possesses some negative partial charge and oxygen atoms are partially negatively charged as expected. In the decomposed structure (Cap^{+2}) the sulfur atom gats partial positive charge although oxygen atoms are still negatively charged but the magnitudes have been comparatively much less (absolutely). In the case of $Cap+Zn^{+2}$ composite the sulfur atom again possesses some negative partial charge as neutral Cap molecule (quite minute in absolute value). Oxygen of OH in COOH group is more negative compared to the oxygens of Cap structure. Also COO-H hydrogen acquires more positive partial charge. All these, as will be displayed in the electrostatic potential map of the

structure (see Figure 4), arises from the zinc cation which gets some electron population from the organic moiety. Hence, the partial positive charge of the zinc cation has been diminished compared to its initial formal charge. Thus, some sorts of redox reactions occur between the components.

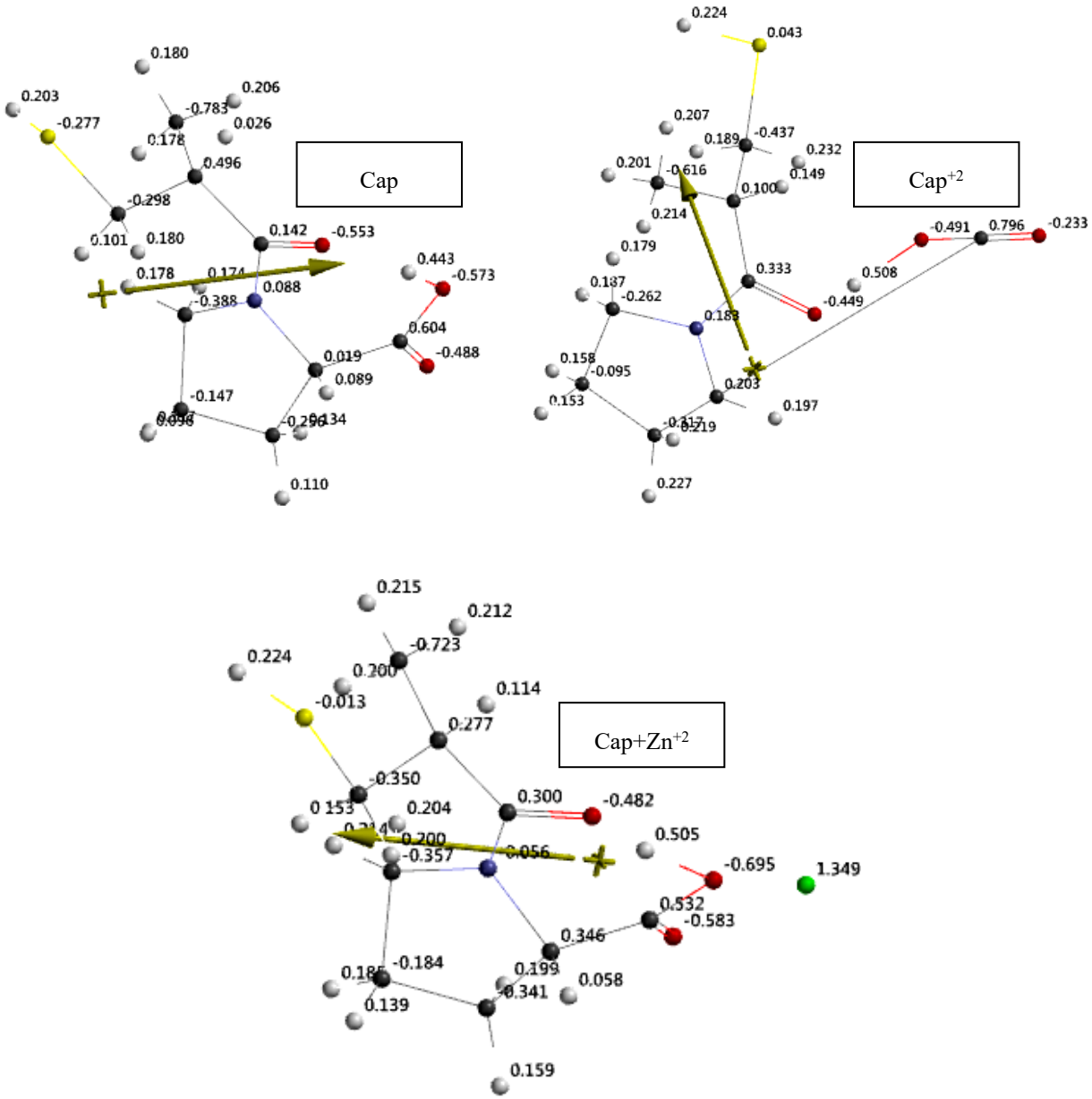

Figure 3. ESP charges on atoms of the species considered.

Electrostatic potential map of the species considered are shown in Figure 4. Note that electro static potential is the energy of interaction of a positive charge with the nuclei and fixed electron distribution of a molecule [27]. In an electrostatic potential map negative potential regions reside on red/reddish and positive ones on blue/bluish parts of the maps. As seen in the figure, the positive charge, (Cap^{+2} and $Cap+Zn^{+2}$) in each case affects the whole molecule, thus the local effects are veiled.

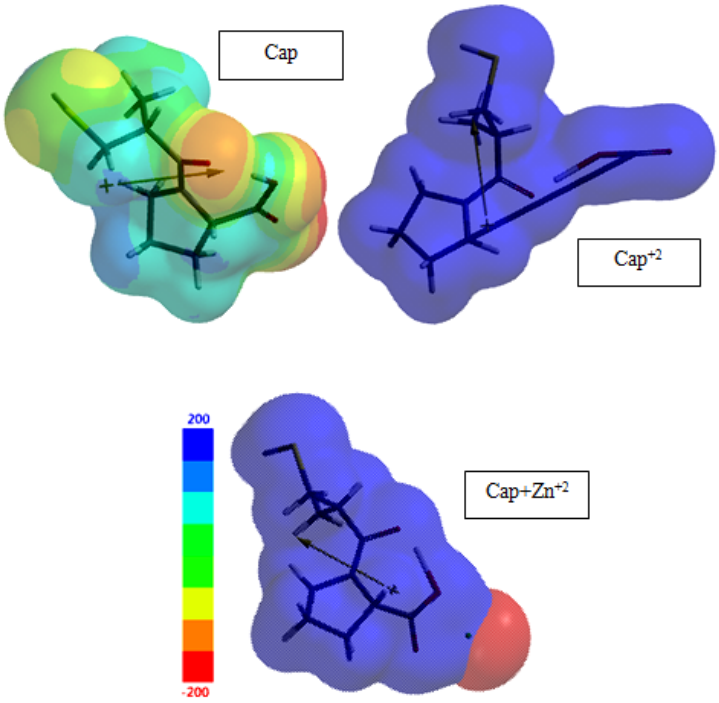

Figure 4. Electrostatic potential map of the species of interest.

Local ionization potential is a measure of the relative ease of electron removal (ionization) as a function of localization [27,28]. Figure 5 shows the local ionization potential maps of the species where conventionally red/reddish regions (if any exists) on the density surface indicate areas from which electron removal is relatively easy, meaning that they are subject to electrophilic attack. Note that the local ionization potential map is a graph of the value of the local ionization potential on an isodensity surface corresponding to a van der Waals surface [27,28].

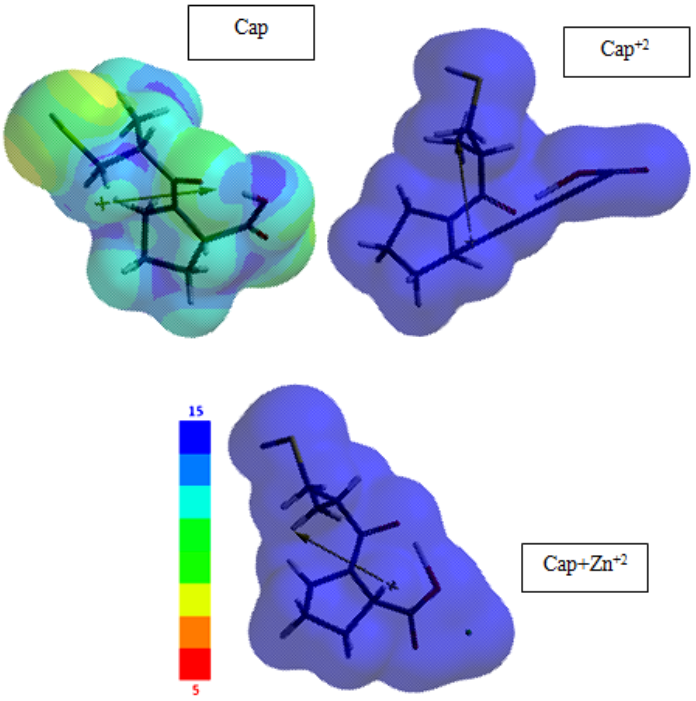

Figure 5. Local ionization potential map of the species of interest.

Figure 6 stands for the LUMO map of the species of interest. Note that a LUMO map displays the absolute value of the LUMO on the electron density surface. The blue color (if any exists) stands for the maximum value of the LUMO and the red colored region, associates with the minimum value. It is to be noted that the LUMO and NEXTLUMO (LUMO+1) are the major orbitals directing the molecule towards the attack of nucleophiles [27,28]. Positions where the greatest LUMO coefficient exists is the most vulnerable site in nucleophilic reactions. Note that in the decomposed structure (Cap^{+2}) the departing moiety has the most red/reddish part).

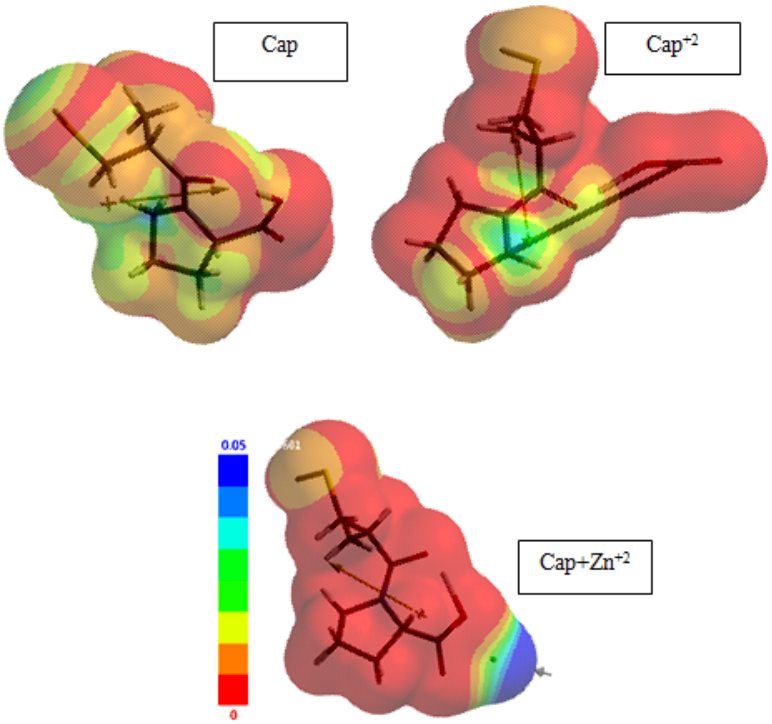

Figure 6. LUMO map of the species of interest.

Figure 7 shows the calculated bond lengths of the species considered. Although, bond lengths vary from structure to structure, as an extreme case, the C-C bond (1.55 Å) of Cap after charging elongates (ruptured) to 6.30 Å in Cap^{+2}.

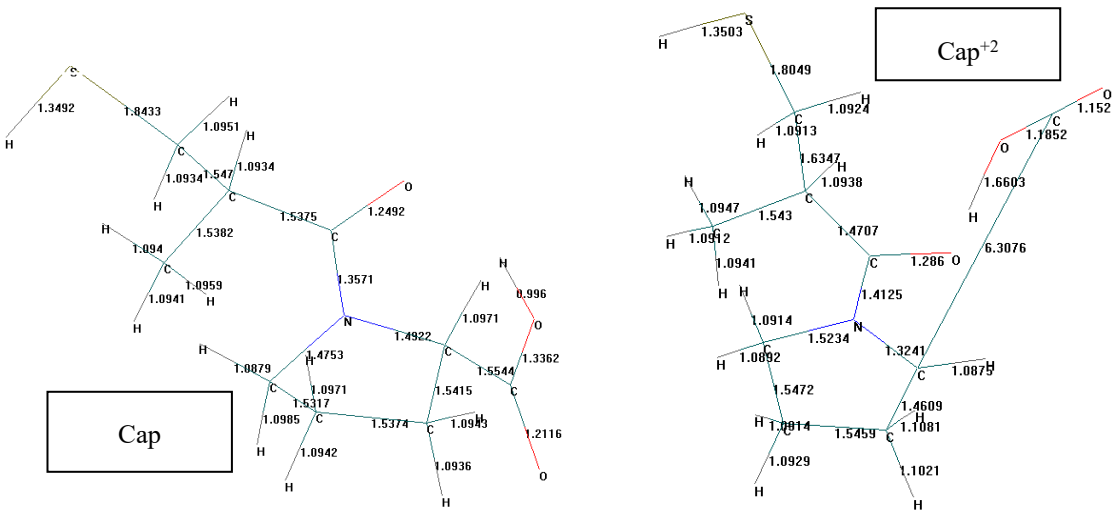

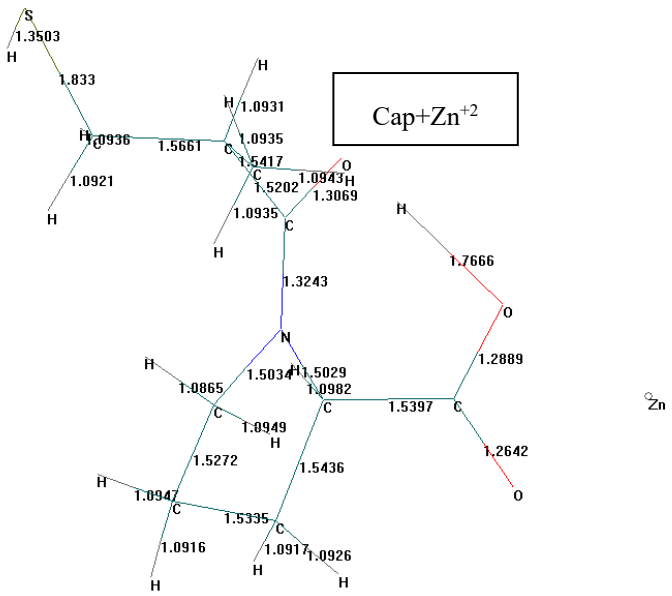

Figure 7. The calculated bond lengths of the species considered.

Figure 8 shows some of the molecular orbital energy levels of the species considered. As seen in the figure, Cap molecule is characterized with a very large HOMO-LUMO energy separation (frontier molecular orbital

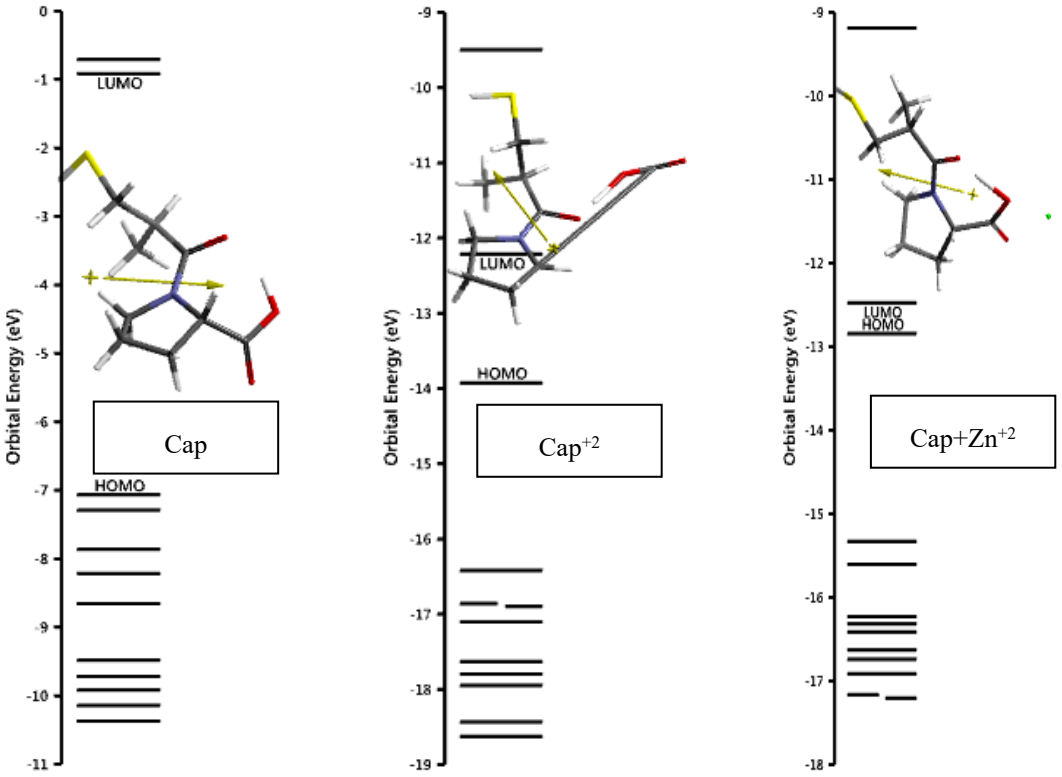

Figure 8. Some of the molecular orbital energy levels of the species considered.

energy gap, $\Delta\varepsilon = \varepsilon_{LUMO}-\varepsilon_{HOMO}$). It decreases going from Cap^{+2} to $Cap+Zn^{+2}$ (see Table 3). So, Zn^{+2} cation, accepting some electron population from Cap molecule (see Figure 2) lowers not only both the HOMO and

LUMO energies of Cap but also the others as well appreciably but at unequal extent to yield energy spectrum of $Cap+Zn^{+2}$ composite. Apparently, the order of Δε values becomes Cap> Cap^{+2}> $Cap+Zn^{+2}$. As will be mentioned in below paragraphs this order affects UV-VIS spectrums of the species of interest.

Table 3 lists the HOMO, LUMO energies and Δε values (in kJ/mol.) of the species considered.

Table 3. The HOMO and LUMO energies and Δε values of the species considered.

Species	HOMO	LUMO	Δε
Cap	-681.89	-88.06	593.83
Cap^{+2}	-1343.52	-1178.51	165.01
$Cap+Zn^{+2}$	-1239.44	-1203.62	35.82

Energies in kJ/mol.

Figure 9 stands for the bond densities of Cap, Cap^{+2} and $Cap+Zn^{+2}$ (composite) considered. Figure clearly indicates that in the case of $Cap+Zn^{+2}$ composite there is a weak interaction between the zinc cation and carboxylic C=O oxygen atom of the organic component. However, some interaction occurs between COO-H and C=O groups of Cap component. All these interactions shuffle the electron population, hence the dipole moment vector of the composite has opposite direction to the respective vector of Cap molecule.

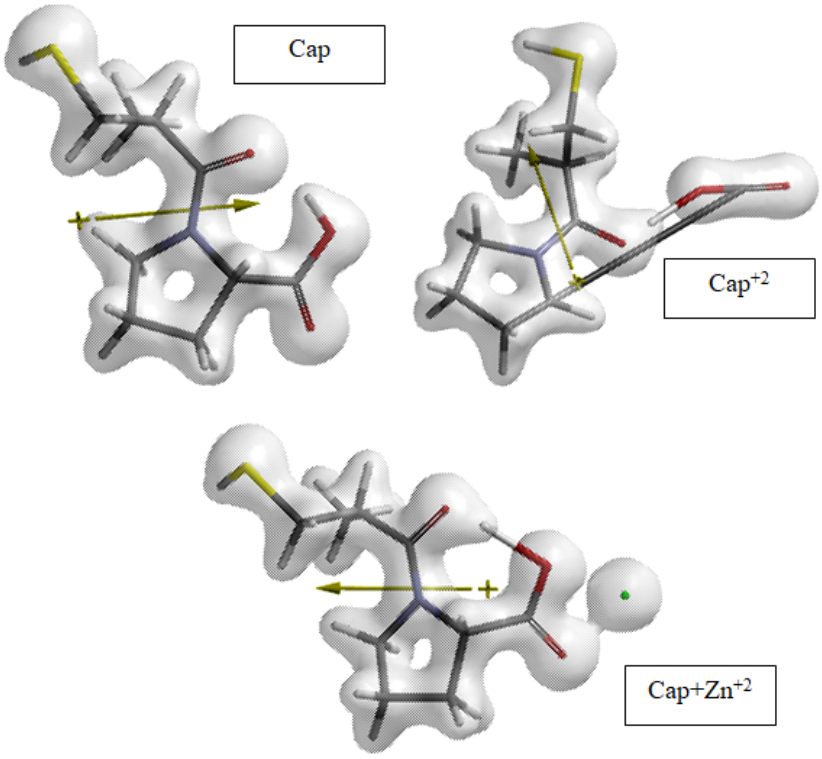

Figure 9. Bond densities of the species considered

Figure 10 shows the UV-VIS spectrums (time dependent density functional, TDDFT) of the species considered. As seen in the figure, Cap spectrum covers rather narrow part of the UV region. Whereas, the spectrum of dication of Cap spreads over the whole UV-VIS region. As for the composite, $Cap+Zn^{+2}$, the spectrum lies over 300-700 nm, having huge peaks and shoulders.

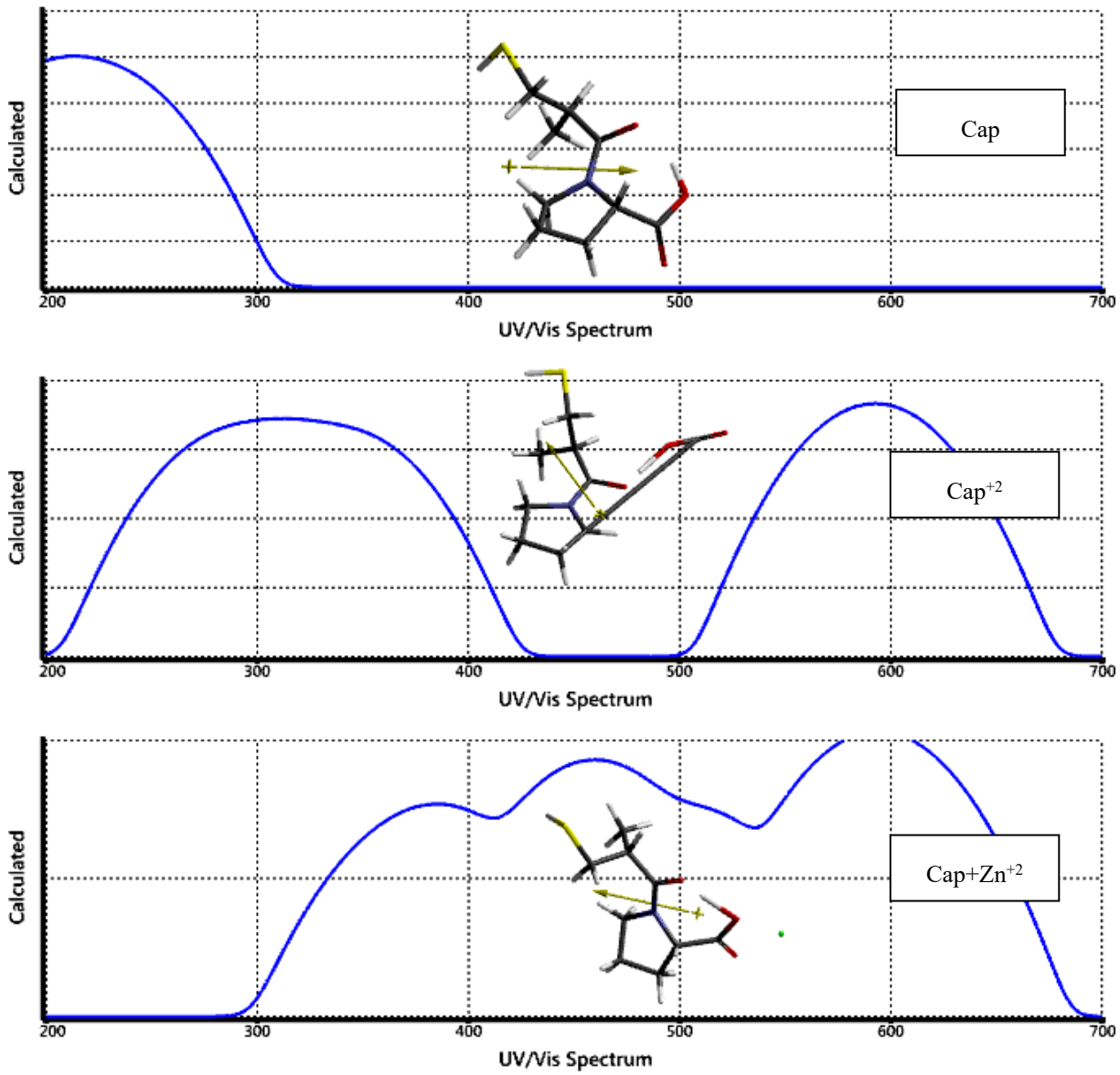

Figure 10. Time dependent density functional UV-VIS spectra of the species of interest.

The order of Δε values is Cap >Cap^{+2}> $Cap+Zn^{+2}$, hence λ_{max} values show pronounced bathochromic shift in the direction of this order. The calculated intensities of the peaks are related to magnitudes of the transition moments between the orbitals involved in the transitions which vary from structure to structure [29,30].

Table 4 lists the λ_{max} values and intensities of the peaks of the spectrums of species of interest.

Table 4. The λ_{max} values and intensities.

Species	λ_{max} (nm)
Cap	206.43 (0.05), 209.96 (0.02), 228.55 (0.026)
Cap^{+2}	314.96 (0.10), 343.72 (0.07), 592.61 (0.31)
$Cap+Zn^{+2}$	388.07 (0.02), 459.75 (0.37), 593.94 (1.56)

The HOMO and LUMO patterns of the species considered are shown in Figure 11. As seen all the species possess π-symmetry. The acid group of Cap structure does not participate in to the HOMO but does in to the LUMO. In all the cases the five memberred ring does not contribute to the HOMO, but has some contribution to

the LUMO of Cap^{+2}. In the case of Cap^{+2} the departing small moiety also does not have any contribution to the HOMO and LUMO.

The zinc cation possesses some small contribution to the HOMO but relatively larger one into the LUMO of the composite, $Cap+Zn^{+2}$.

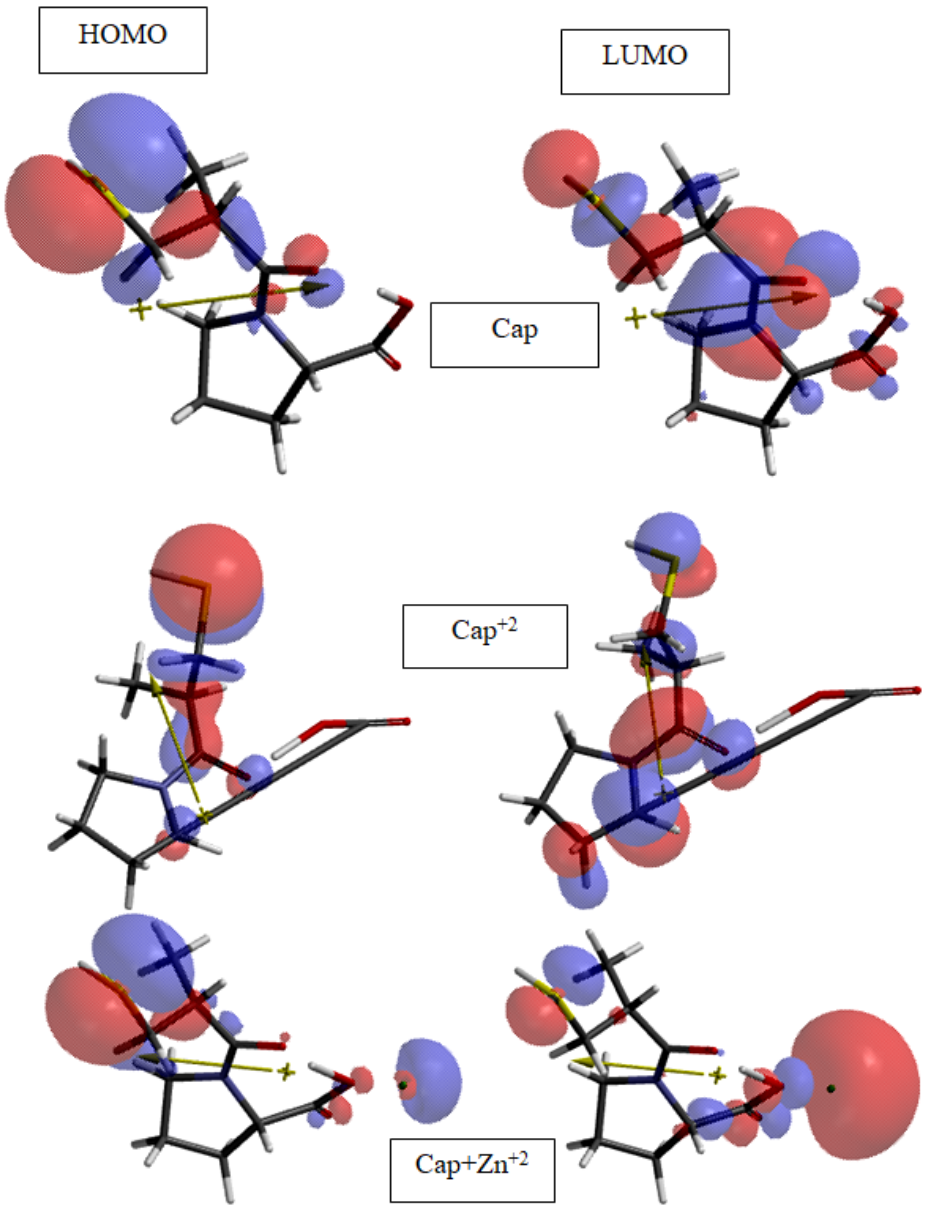

Figure 11. The HOMO and LUMO patterns of the species considered.

Table 5 lists some properties of the species of interest. The dipole moment values of the species are the vectorial sum of bond dipoles which is dependent on the charges and bond lengths and note that among the structures considered Cap^{+2} has the minimum whereas $Cap+Zn^{+2}$ has the maximum value of the dipole moment.

As for the log P values, partition coefficients are important property and useful in estimating the distribution of drugs within the body. Hydrophobic drugs with high octanol-water partition coefficients are mainly distributed to hydrophobic areas such as lipid bilayers of cells. Conversely, hydrophilic drugs (low octanol/water partition coefficients) are found primarily in aqueous regions such as blood serum.

Table 5. Some properties of the species of interest.

Species	Dipole moment	Polarizability	Area (Å²)	Volume (Å³)	Ovality	Log P	Cv (J/molº)
Cap	6.16	57.02	232.56	210.79	1.36	0.24	166.72
Cap^{+2}	3.41	58.93	257.34	221.38	1.45	0.24	172.94
$Cap+Zn^{+2}$	16.97	58.90	242.43	217.09	1.39	-	180.11

Dipole moments in debye units. Polarizabilities in 10^{-30} m^3 units.

4. Conclusion

The computational study presently considered, deals with Cap, its statically-charged dication form (Cap^{+2}) and $Cap+Zn^{+2}$ composite within the restrictions of density functional theory at the level of B3LYP/6-31+G(d). All of the species considered possess exothermic Hº and favorable Gº values and as well as they are electronically stable. In the composite, as most of the properties, their HOMO and LUMO energies are dictated by the fine topology of the structures considered. However, the smallest Δε value is associated with the composite in which zinc cation gets some electron population from the organic moiety and thus itself has been reduced.

All these points are to be investigated by clinical experiments to search the effect of Cap in the zinc or zinc associated metabolisms in its long period of usage.

References

[1] Tapiero, H., & Tew, K. D. (2003). Trace elements in human physiology and pathology: Zinc and metallothioneins. *Biomedicine & Pharmacotherapy, 57*(9), 399–411. https://doi.org/10.1016/S0753-3322(03)00081-7

[2] Maret, W. (2011). Metals on the move: Zinc ions in cellular regulation and in the coordination dynamics of zinc proteins. *BioMetals, 24*(3), 411–418. https://doi.org/10.1007/s10534-010-9406-1

[3] Fenton, D. E. (1993). *Biocoordination chemistry* (Oxford Chemistry Primers, No. 26). Oxford University Press.

[4] Mocchegiani, E., Bertoni-Freddari, C., Marcellini, F., & Malavolta, M. (2005). Brain, aging and neurodegeneration: Role of zinc ion availability. *Progress in Neurobiology, 75*(6), 367–390. https://doi.org/10.1016/j.pneurobio.2005.04.005

[5] Maret, W. (2013). Zinc and human disease. In A. Sigel, H. Sigel, & R. O. Sigel (Eds.), *Interrelations between essential metal ions and human diseases* (Metal Ions in Life Sciences, Vol. 13, pp. 389–414). Springer. https://doi.org/10.1007/978-94-007-7500-8_12

[6] Hausman, P. (1987). *The right dose: How to take vitamins and minerals safely*. Ballantine Books.

[7] Heel, R. C., Brogden, R. N., Speight, T. M., & Avery, G. S. (1980). Captopril: A preliminary review of its pharmacological properties and therapeutic efficacy. *Drugs, 20*(6), 409–452. https://doi.org/10.2165/00003495-198020060-00001

[8] Benowitz, N. L., & Bourne, H. R. (1984). Antihypertensive agents. In B. G. Katzung (Ed.), *Basic and clinical pharmacology* (2nd ed., pp. 134–153). Lange Medical Publications.

[9] Frohlich, E. D., Cooper, R. A., & Lewis, E. J. (1984). Review of the overall experience of captopril in hypertension. *Archives of Internal Medicine, 144*(7), 1441–1444. https://doi.org/10.1001/archinte.1984.00350190137023

[10] Fouad, A. A., Al-Mulhim, A. S., Jresat, I., & Morsy, M. A. (2013). Protective effects of captopril in diabetic rats exposed to ischemia/reperfusion renal injury. *Journal of Pharmacy and Pharmacology, 65*(2), 243–252. https://doi.org/10.1111/j.2042-7158.2012.01585.x

[11] Nagasawa, T. H., Khan, M. A., & Imig, J. D. (2012). Captopril attenuates hypertension and renal injury induced by the vascular endothelial growth factor inhibitor sorafenib. *Clinical and Experimental Pharmacology and Physiology, 39*(5), 454–461. https://doi.org/10.1111/j.1440-1681.2012.05699.x

[12] Dondi, M., Franchi, R., Levorato, M., Zuccala, A., Gaggi, R., Mirelli, M., Stella, A., Marchetta, F., Losinno, F., & Monetti, N. (1989). Evaluation of hypertensive patients by means of captopril enhanced renal scintigraphy with technetium-99m DTPA. *Journal of Nuclear Medicine, 30*(5), 615–621.

[13] Geyskes, G. G., Oei, H. Y., Puylaert, C. B., & Mees, E. J. (1987). Renovascular hypertension identified by captopril-induced changes in the renogram. *Hypertension, 9*(5), 451–458. https://doi.org/10.1161/01.hyp.9.5.451

[14] Mann, S. J., Pickering, T. G., Sos, T. A., Uzzo, R. G., Sarkar, S., Friend, K., Rackson, M. E., & Laragh, J. H. (1991). Captopril renography in the diagnosis of renal artery stenosis: Accuracy and limitations. *American Journal of Medicine, 90*(1), 30–40. https://doi.org/10.1016/0002-9343(91)90503-P

[15] Oei, H. Y., Geyskes, G. G., Mees, E. J., & Puylaert, C. B. (1987). The significance of captopril renography in renovascular hypertension. *Contributions to Nephrology, 56*, 95–103. https://doi.org/10.1159/000413788

[16] Setaro, J. F., Saddler, M. C., Chen, C. C., Hoffer, P. B., Roer, D. A., Markowitz, D. M., Meier, G. H., Gusberg, R. J., & Black, H. R. (1991). Simplified captopril renography in diagnosis and treatment of renal artery stenosis. *Hypertension, 18*(3), 289–298. https://doi.org/10.1161/01.hyp.18.3.289

[17] Sfakianakis, G. N., Bourgoignie, J. J., & Jaffe, D. (1987). Single-dose captopril scintigraphy in the diagnosis of renovascular hypertension. *Journal of Nuclear Medicine, 28*(9), 1383–1392.

[18] Bolterman, R. J., Manriquez, M. C., Ruiz, M. C. O., Juncos, L. A., & Romero, J. C. (2005). Effects of captopril on the renin angiotensin system, oxidative stress, and endothelin in normal and hypertensive rats. *Hypertension, 46*(4), 943–947. https://doi.org/10.1161/01.HYP.0000174602.59935.d5

[19] Stewart, J. J. P. (1989). Optimization of parameters for semi-empirical methods I. *Journal of Computational Chemistry, 10*(2), 209–220. https://doi.org/10.1002/jcc.540100208

[20] Stewart, J. J. P. (1989). Optimization of parameters for semi-empirical methods II. *Journal of Computational Chemistry, 10*(2), 221–264. https://doi.org/10.1002/jcc.540100209

[21] Leach, A. R. (1997). *Molecular modeling*. Longman.

[22] Kohn, W., & Sham, L. J. (1965). Self-consistent equations including exchange and correlation effects. *Physical Review, 140*(4A), 1133–1138. https://doi.org/10.1103/PhysRev.140.A1133

[23] Parr, R. G., & Yang, W. (1989). *Density functional theory of atoms and molecules*. Oxford University Press.

[24] Becke, A. D. (1988). Density-functional exchange-energy approximation with correct asymptotic behavior. *Physical Review A, 38*(6), 3098–3100. https://doi.org/10.1103/PhysRevA.38.3098

[25] Vosko, S. H., Wilk, L., & Nusair, M. (1980). Accurate spin-dependent electron liquid correlation energies for local spin density calculations: A critical analysis. *Canadian Journal of Physics, 58*(8), 1200–1211. https://doi.org/10.1139/p80-159

[26] Lee, C., Yang, W., & Parr, R. G. (1988). Development of the Colle-Salvetti correlation energy formula into a functional of the electron density. *Physical Review B, 37*(2), 785–789. https://doi.org/10.1103/PhysRevB.37.785

[27] Wavefunction Inc. (2006). SPARTAN 06 (Version 1.0). Wavefunction Inc.

[28] Wavefunction Inc. (2006). TRIDENT: Molecular modeling for medicinal chemists. Wavefunction Inc.

[29] Turro, N. J. (1991). *Modern molecular photochemistry*. University Science Books.

[30] Anslyn, E. V., & Dougherty, D. A. (2006). *Modern physical organic chemistry*. University Science Books.